EUVE SCIENCE PAYLOAD AND INSTRUMENTATION

2.1 Science Payload Configuration

The physical configuration of the science payload is illustrated in figure 1-1, along with the coordinate system frequently used to refer to the science payload and spacecraft. The three scanning instruments are stacked to point along the spacecraft -Y axis, which is the DS/S X axis. The DS/S points away from the PED along the spacecraft -X axis. This is also the DS/S Z axis and the spacecraft spin axis in sky-survey mode.

2.2 The EUVE Spectrometer

The instruments designed for the EUVE mission are the product of over two decades of development by the Space Astrophysics Group in Berkeley. This section will describe the EUVE Spectrometer by first describing its components and then the complete system and its calibration. The Deep Survey instrument will also be described, as some data from the Deep Survey are routinely provided to Guest Observers.

The Spectrometer is a three-fold symmetric slitless objective design based on variable line space grazing incidence reflection gratings. Photon images are accumulated simultaneously in three bandpasses with effective spectral resolutions of $\lambda/\Delta\lambda \sim 200$–$400$ in 3 bandpasses from 70–760 Å. The instrument is pictured in cross section in figure 2-1, and its physical characteristics are summarized in table 2-2. The Spectrometer and Deep Survey instruments share the DS/S mirror. The regions of the mirror devoted to the Spectrometer and Deep Survey are defined at the front aperture, which is an annulus divided into six segments. Each of the Spectrometer channels receives a beam of light from one of three alternating segments. This division gives each channel a geometric area of ~ 75 cm^2. After the mirror, each converging beam then strikes one of three gratings which focus the spectra onto three detectors, arranged in a circle around the central Deep Survey detector.

The throughput of the EUVE Spectrometer is determined by the combined effects of the mirrors' and gratings' coating reflectivities, which are functions of both wavelength and grazing angle, the filter transmissions, and the quantum efficiency functions of the detector photocathode materials.

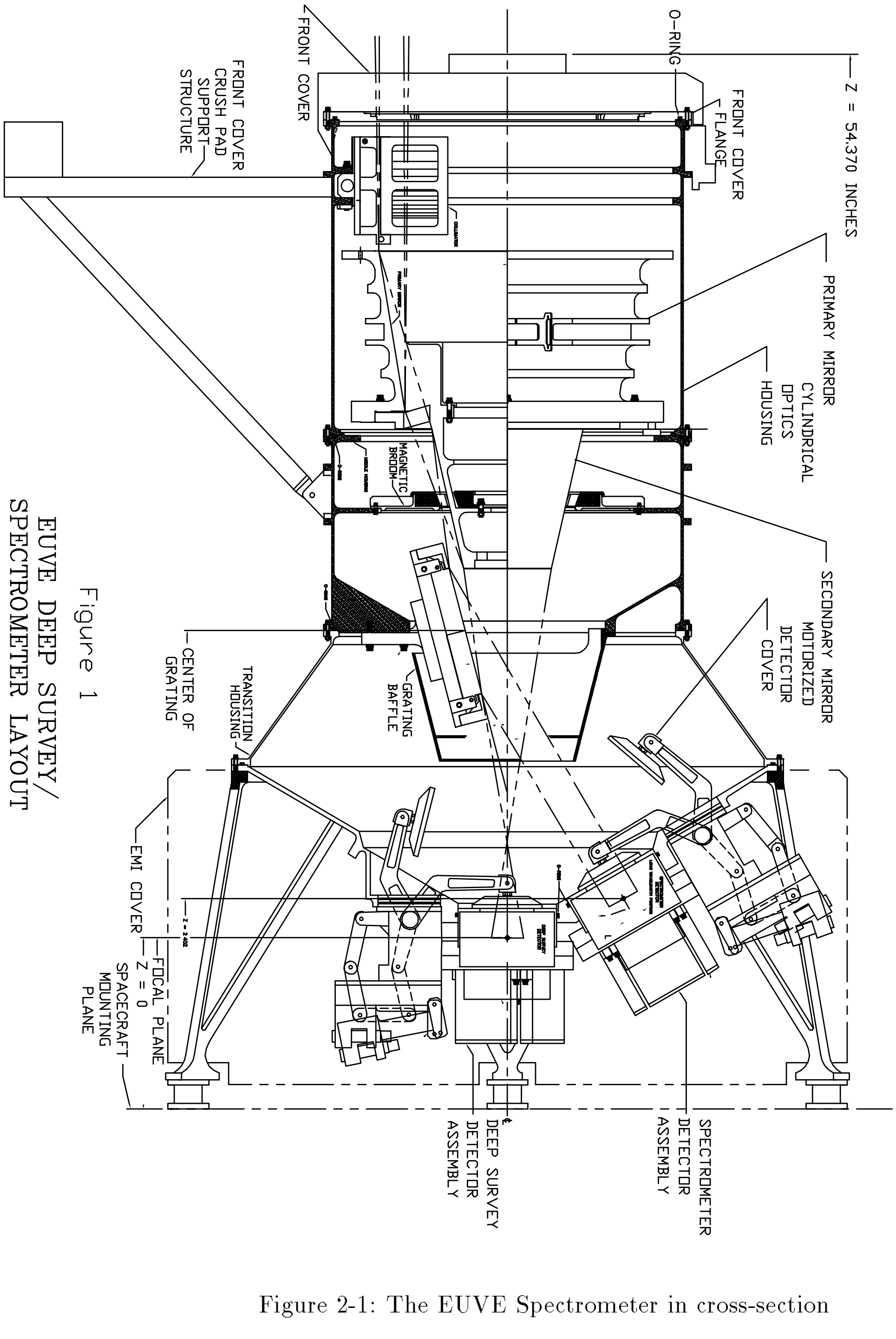

Figure 2-1: The EUVE Spectrometer in cross-section

2.2.0.1 The DS/S Telescope

Mirror reflectivities in the EUV are generally maximized by the use of grazing incidence optics. All the EUVE instruments employ polished metal grazing incidence mirrors, which provide very compact imaging systems with relatively large fields of view, and adapt well to the stringent requirements of space platforms.

The DS/S telescope is a Wolter-Schwarzschild Type II design, with a concave primary and a convex secondary. The mirror has a focal length of 136 cm and is f/3.3, with a total geometric area of over 450 cm^2. The primary and secondary mirrors are both gold-coated. Characteristics of the optic are summarized in table 2-1. Reflectivity tests were performed on the finished mirror, using light between 44 Å and 1216 Å. The results are shown in figure 2-2.

Table 2-1: The DS/S Mirror

Focal Length	136.242 cm
f/ratio	3.3
Geometric Area	452.97 cm^2
Field of View	2° diameter
Average Graze Angles (primary, secondary)	9°, 5.5°
Surface coating	sputtered Au, $\sim$ 350 Å
FWHM (Optical)	$1.6\,''$
HEW (Optical)	$12\,''$

The point spread function and the half energy width and scattering of the mirrors have been measured at Berkeley's EUV calibration facilities [4] to assure acceptable standards of imaging.

Measurements of the point spread function in the EUV give the angular resolution at the center of the field of view as approximately 18 arc seconds. When coupled to a 50 mm EUVE MCP detector, this produces and instrument plate scale of 6.60 μ per arc second. The focused image size at optical wavelengths is about 12 arc seconds' half-energy width (HEW) after polishing.

The mirror collects light through an annular aperture divided into six segments. Three segments feed the Deep Survey imaging system, which is described further in section 2.3. Baffles before the telescope, near the midpoints of the primary and secondary mirrors, and side baffles on the grating assemblies help exclude diffuse geocoronal radiation from the telescope and scattered light from all the detectors. To exclude charged particles, the telescope is equipped with a magnetic broom, between the secondary baffle and secondary mirror. It is designed to divert electrons with energies up to 15 kV, and thermal ions with energies up to .3 eV. Each detector is also protected by a 10 Newton repellor grid, biased to 28 V.

2.2.1 Collimators and Sky Background

In order to achieve good spectral resolution, any EUV spectrometer must be designed to limit the effect of diffuse sky radiation. The medium and long wavelength channels of the EUVE Spectrometer have wire-grid collimators placed directly after the aperture before the mirror, which limit the grazing angles of the incident light to exclude some of the sky background. They consist of 15 etched molybdenum grids, spaced exponentially and held in a thermally stable claw structure, also of molybdenum. The transmission profile of the stack is triangular in the dispersion direction, and limits the beam to 20 arc minutes FWHM.

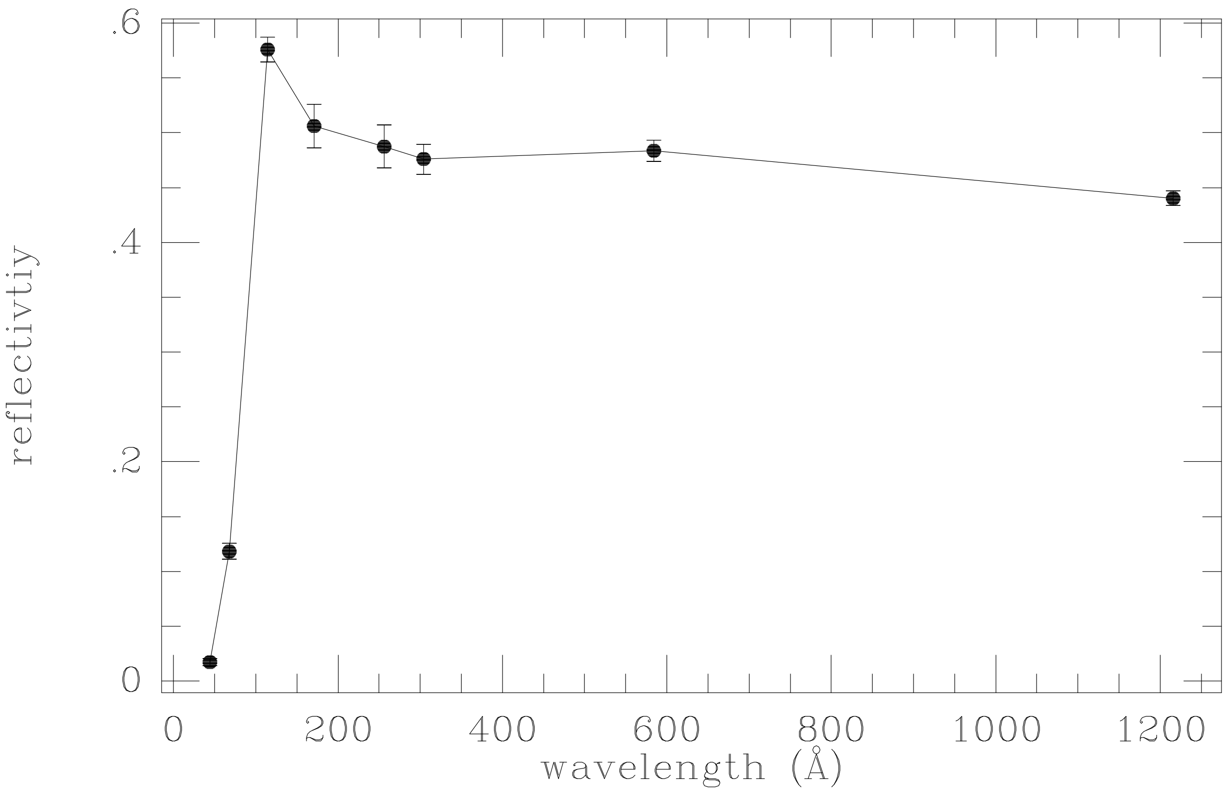

Figure 2-2: DS/S mirror reflectivity in the EUV

The transmission of of each collimator assembly was tested in visible light. The collimator relative transmissions were measured in the EUV by comparing the Spectrometer throughputs, measured as a function of off-axis angle, before and after installation of the collimators in the medium and long wavelength channels. Alignment to the boresight of the instrument was also determined. Both collimators function as designed, with peak transmissions of 64.2% and 65.4% in the medium and long wavelength channels, respectively. Figure 2-3 illustrates the collimator relative transmission measured in the long wavelength channel. Relative transmission is the ratio of Spectrometer channel throughput with the collimator installed to that measured without the collimator.

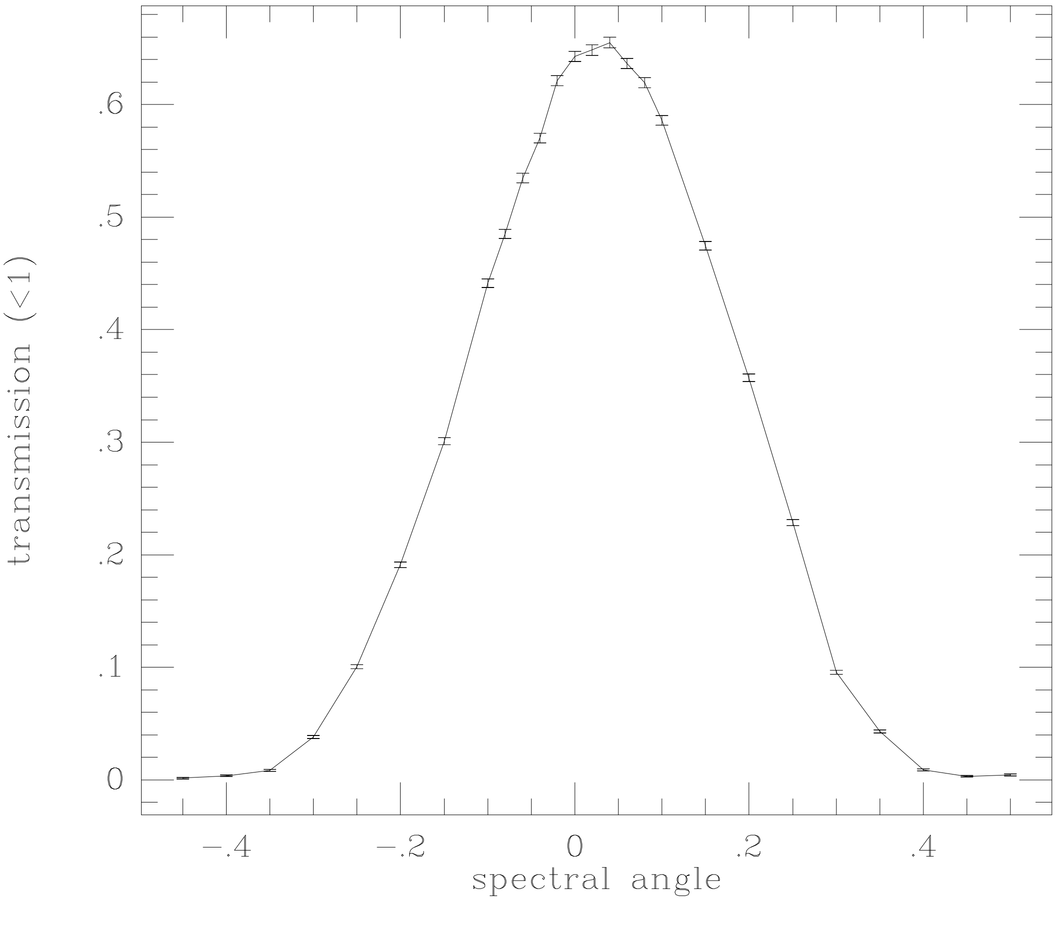

Figure 2-3: Long Wavelength collimator transmission

2.2.2 Variable Line Space Gratings

The EUVE Spectrometer incorporates plane diffraction gratings with continuously varying line spacing, placed in the converging beam of the telescope to diffract the light as it approaches the focus. Like concave gratings, they obviate the use of other focusing optics after dispersion. Unlike uniformly spaced rulings, variable line space gratings can produce nearly stigmatic spectra using straight, conventionally ruled grooves [13],[12].

The gratings are blazed for use in the first inside order. "Inside" will be used to mean diffracted orders at angles between the surface normal and the specular direction, and will be referred to with a minus sign when represented numerically, e.g. -1st order. The gratings cover three overlapping bandpasses; short wavelengths from 70 to 190 Å, medium wavelengths from 140 to 380 Å, and long wavelengths from 280 to 760 Å. The groove densities range from 415 to 3550 grooves/mm. The gratings were ruled by Hitachi, Inc. at the Naka optical works in Japan. The short wavelength grating is coated with rhodium to optimize the reflectivity between 70 and 190 Å. The medium and long wavelength gratings have platinum surface coatings.

2.2.3 Spectrometer Filters

Thin film filters, a few thousand Å thick, completely cover each detector. They define broad bandpasses while screening out bright geocoronal and interplanetary lines such as Lyman alpha radiation and some higher orders of diffraction. The Spectrometer filter configuration is shown in figure 2-4. The materials are Lexan and boron in the short wavelength, aluminum and carbon in the medium, and aluminum in the long wavelength channel. The measured transmissions for the Spectrometer Lexan and aluminum filter materials are plotted in figures 2-5 and 2-6 in both log and linear coordinates. Material thicknesses are included in table 2-2.

The two longer wavelength filters have an off-axis quadrant[1] of material which covers the same bandpass as one of the shorter channels. At these positions, which correspond to off-axis angles of approximately 0.5°, some wavelengths that would normally lie in the shorter channel's range appear in the longer wavelength channel in second order ($n = -2$), and are passed by the alternate filter. Wavelengths from parts of the shorter bandpass that overlap the longer channel also appear in first order. These off-axis locations are configured to be used as backups to duplicate the short and medium channels, should either of these detectors fail.

2.2.4 Microchannel Plate Detectors

All the EUVE detectors are Microchannel plate (MCP) detectors. MCP detectors are electron-amplification devices that provide two-dimensional imaging and time-tagging of individual EUV photon events [25, 28].

[1] The sections of a filter are numbered from 0 and referred to as quadrants, regardless of the number of sections in any one filter.

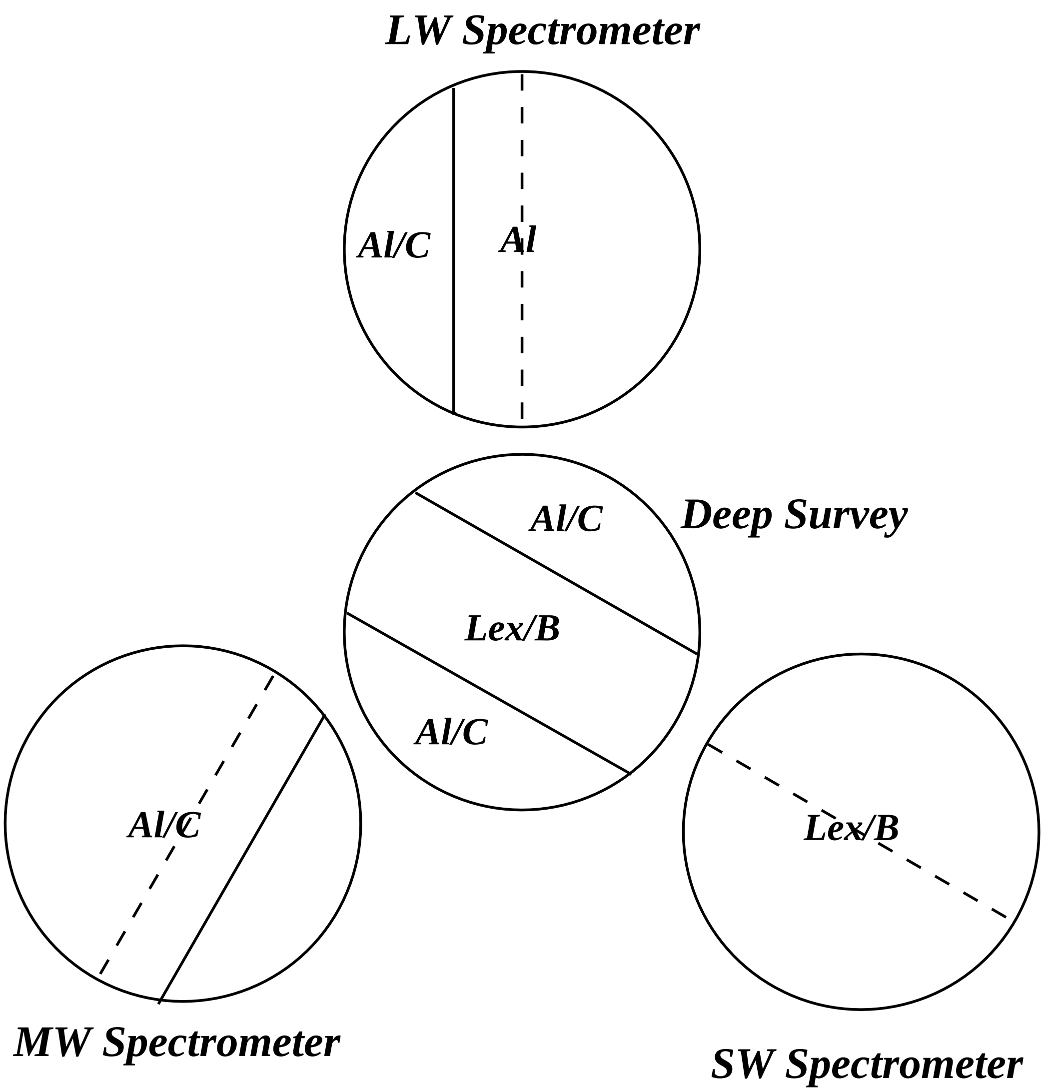

Figure 2-4: Spectrometer filter configuration. Dashed lines show orientation of spectra.

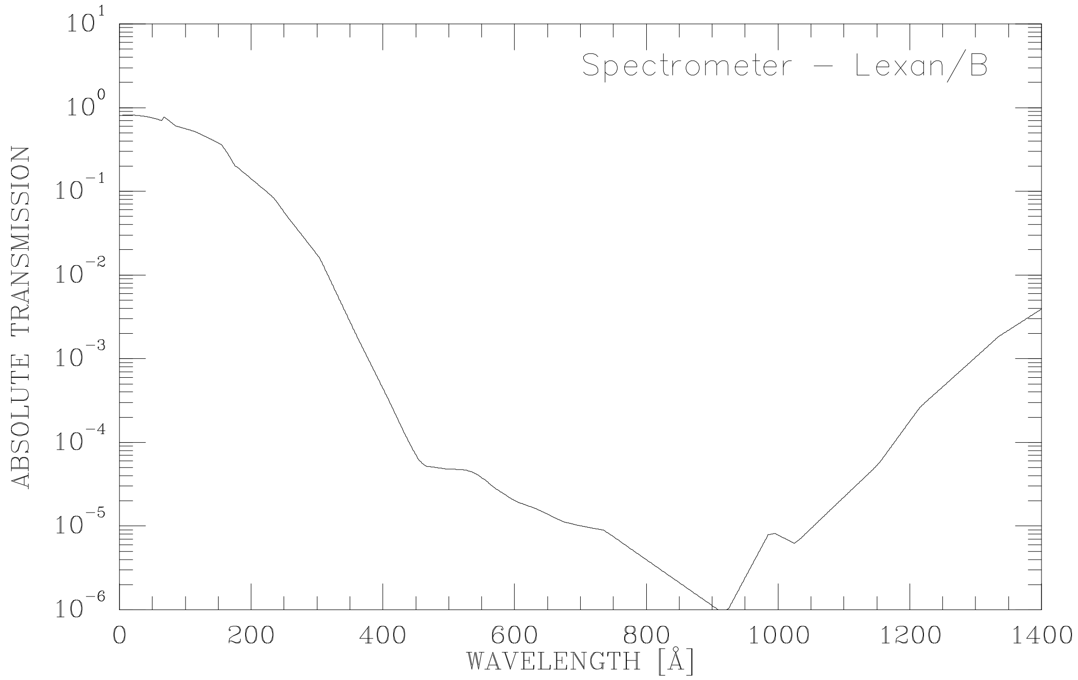

Figure 2-5: a) Spectrometer Lexan filter transmissions. Log scale.

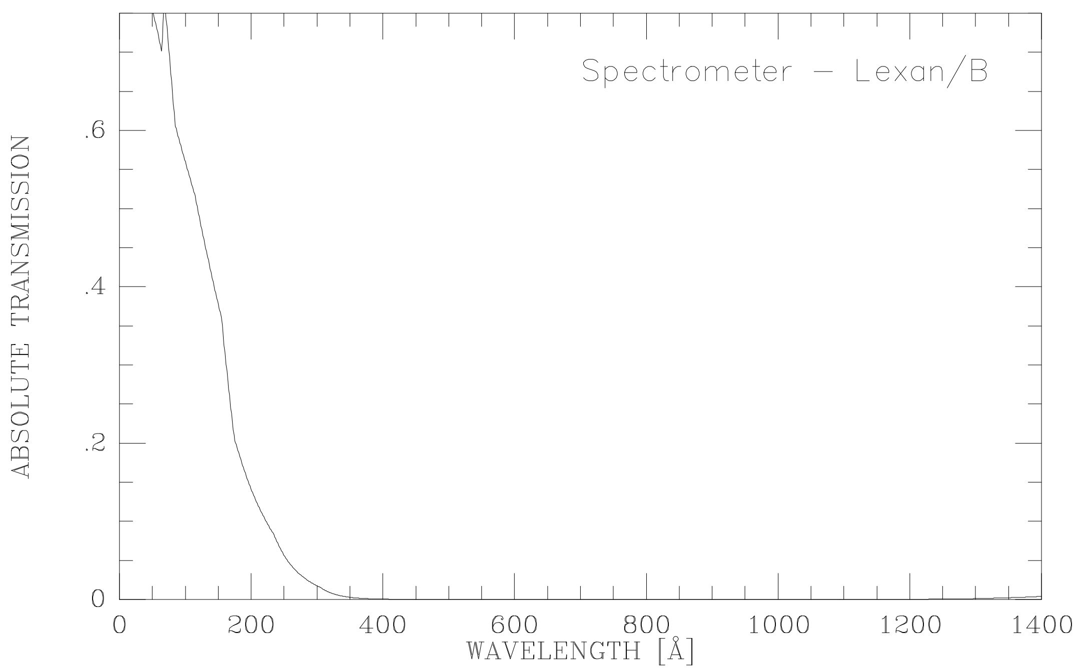

Figure 2-5: b) Spectrometer Lexan transmission. Linear scale.

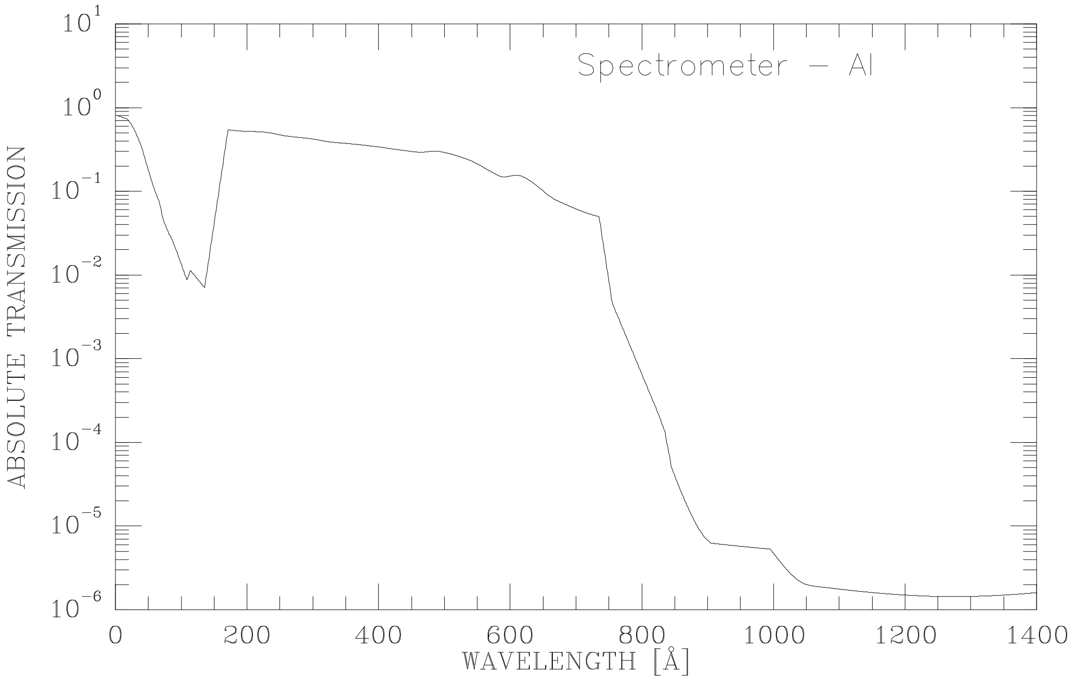

Figure 2-6: a) Spectrometer aluminum filter transmissions. Log scale.

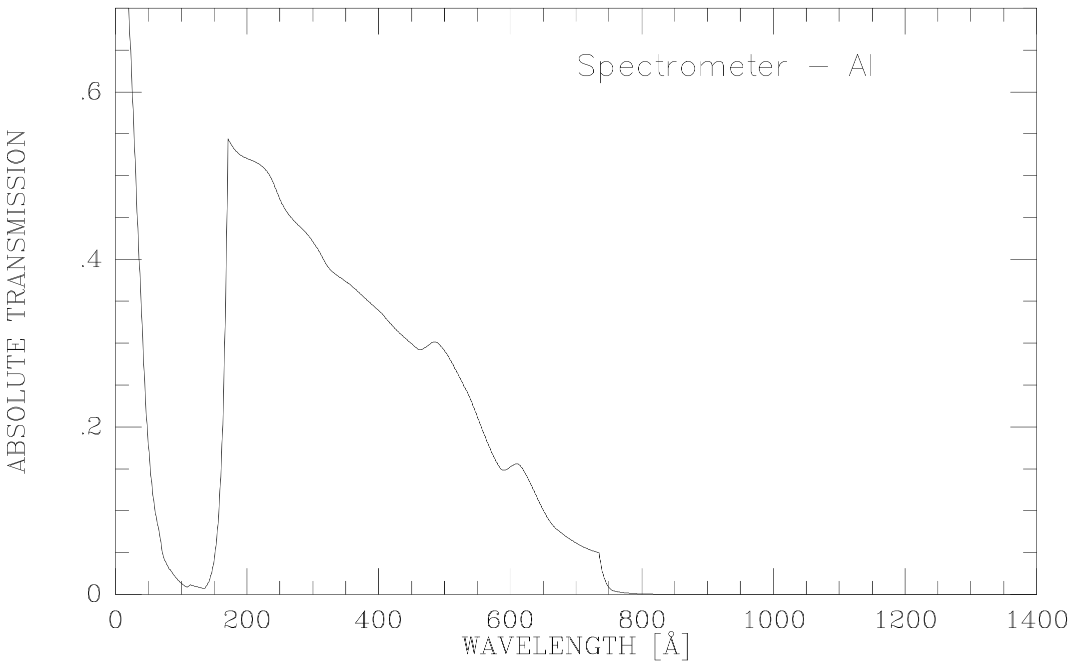

Figure 2-6: b) Spectrometer aluminum transmission. Linear scale.

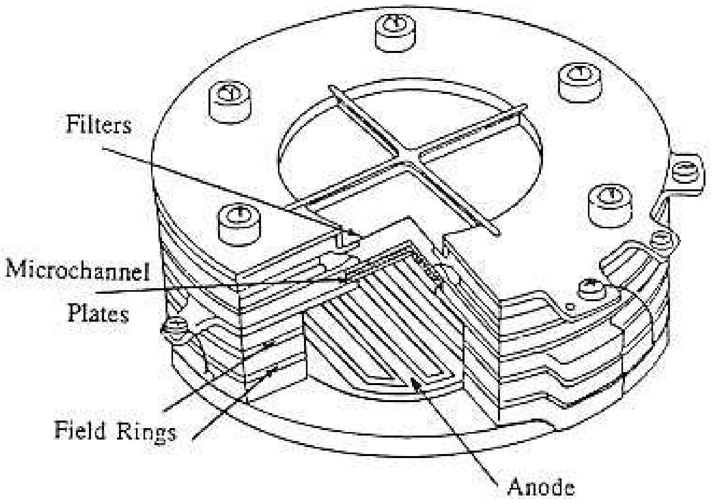

Figure 2-7: Cut away view of EUVE detector.

Figure 2-7 shows a cut-away view of a typical EUVE scanner detector. The Spectrometer has three MCP detectors, arranged at 120° intervals around the central Deep Survey detector. Recall that the Spectrometer filter design is shown in figure 2-4.

Each detector employs a biased stack of three porous quartz MCP's with a channel-length-to-diameter ratio of approximately 80:1. The stack acts as an electron multiplier, and is backed by a conducting anode, partitioned into a graduated "wedge, strip, and zigzag" pattern (see Figure 2-8). The top plate has an applied photocathode of potassium bromide (KBr) [21], to enhance the photoelectric response at EUV wavelengths. When a photon excites the front surface, a bias of 4-5 kV causes cascading electrons to form a cloud of 2-3$\times 10^7$ e^- which then strikes the divided anode.

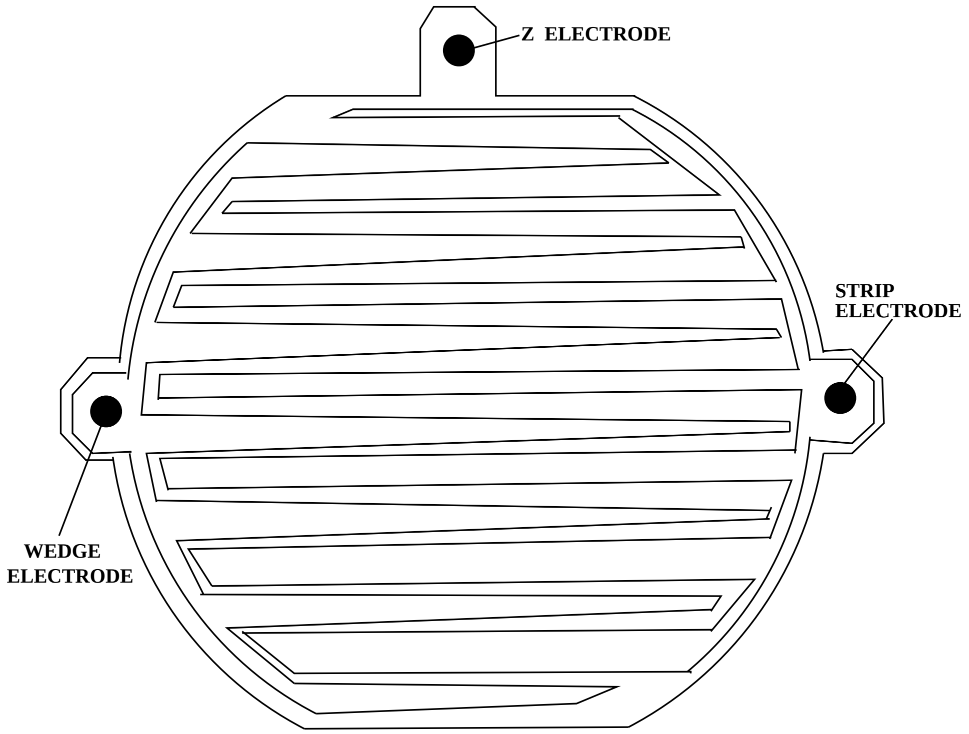

Figure 2-8: Wedge and strip anode pattern for MCP detector.

Event positions (X,Y) are calculated by on-board instrument software (ISW) from the division of the charge cloud among the wedge, strip, and zigzag areas of the anode. The detectors record positions $0 - 2047$ in each dimension, and a single pixel is about $29 \times 29\mu$. This results in a pixel size of roughly $4.25\widehat{''}$ when remapped to the sky.

All the detectors are equipped with four stimpulser, or "stim" pins, which periodically excite the anode at standard positions, and are used to monitor position stability. The detectors have been placed at the sagittal intersection to produce good imaging over the whole detector, rather than optimized spectral focus at one point.

MCP Fixed Pattern Noise

It has been known for some time that the EUVE spectrometer detectors exhibit a characteristic fixed pattern noise that produces quasi-periodic modulations in continuum spectra. This effect is caused by event locations being shifted near the boundaries of the "bundles" of quartz tubes which make up the MCP's.
A microchannel plate is a cross-section of many bundles of thin quartz tubes. The the bundles are packed together in a hexagonal pattern to make the microchannel boule. In the process, the areas at the edges of the bundles tend to get a few flattened tubes. In the finished microchannel plate, the deformed bundle borders form a regular hexagonal pattern where the surface has more "wall" than "hole".
When a photon event creates an electron cascade in the channel plates, the center of the electron cloud may be displaced if it falls on distorted channels, especially if this happens in the last plate, just before the cloud strikes the anode. Flux is conserved, but events are shifted away from the (regularly spaced) bundle borders. Shifts can occur in either the spectral or the imaging direction. A net modulation of 10 - 20% can be observed in continuum spectra on a scale of 16–20 pixels if enough events are accumulated.
This effect can cause spurious absorption or emission features to appear, and can displace existing line centers. The effect is most noticeable and troubling in observations of bright continuum sources, such as white dwarf stars. The observing strategy used to minimize this effect is usually referred to as "dithering", and is described in sections 3.3 and 4.2.

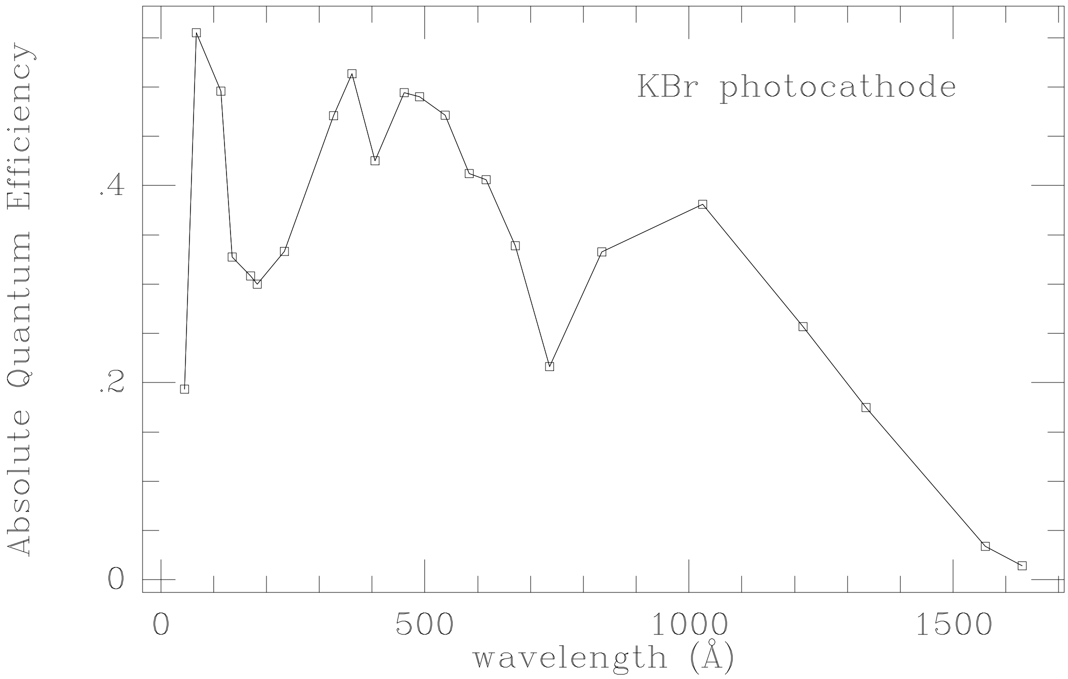

Figure 2-9: KBr photocathode QE for Spectrometer detector.

The quantum efficiency of each photocathode was measured at various EUV wavelengths. An example set of measurements is shown in figure 2-9. Spectral and angular resolution are both addressed quantitatively in chapter 3.

Table 2-2: The EUVE Spectrometer

	Short λ	**Medium λ**	**Long λ**
bandpass	70–190 Å	140–380 Å	280–760 Å
geometric area	72.44 cm^2	72.44 cm^2	72.44 cm^2
resolution element ($\Delta\lambda$)	0.367 – 0.636Å	0.731 – 1.27Å	1.46 – 2.54Å
collimator FWHM (spectral direction)	none	$20'$	$20'$
grating optical coating	rhodium	platinum	platinum
filter material	Lexan/boron 1588Å/1172Å	Al/carbon 1566Å/431Å	aluminum 1553Å
detector diameter	50 mm $5° \times 2°$	50 mm $5° \times 2°$	50 mm $5° \times 2°$
photocathode material	KBr	KBr	KBr

2.2.4.1 Instrument Electronics

Each detector in the science payload is supported by a separate set of amplifiers and analog-to-digital converters (ADCs), which convert the charge cloud partitions into pulses and calculate the X-Y coordinates of each photon event.

A separate telescope interface (TIF) unit handles logical switching and photon event data for each detector, and a relay interface (RIF) unit, controls power switching for the detector and mechanical door.

Data from all the detectors is processed by a central command, data, and power unit (CDP), which transmits photon data, commands and engineering information between the science payload and the spacecraft. The CDP also controls the spacecraft power interface via a redundant Remote Interface Unit (RIU). The simplified block diagram of the EUVE science payload in figure 2-10 shows the parallelism of the TIF's, and the redundant CDP modules.

Photon events in the several quadrants on each detector are input to telemetry (TM) by means of an algorithm called "primbsching", executed in the CDP, that allocates equal weight to events from each quadrant of the operating detectors. The algorithm guarantees an equal number of event "slots" to each quadrant; this prevents a single bandpass with high backgrounds from saturating the tes. The telemetry can transmit up to 437 events per second from any combination of the satellite detectors.

2.2.5 Spectrometer Calibration

This section gives a qualitative account of the the Spectrometer calibration, to acquaint users with the current level of knowledge about the instrument. Quantitative results of measurements and useful characteristic functions are given in chapter 3. New results are made available periodically through the CEA/EUVE *ftp* site and the NASA ADS, and referenced in the literature as they are produced.

The performance of each individual component for the EUVE science payload was tested in the vacuum ultraviolet calibration facility at Berkeley. Tests of the fully assembled Spectrometer measured effective area and order efficiency as a function of wavelength, imaging under various temperature conditions, and spectral resolution. The tests employed both monochromatic light and full spectra from several sources of EUV light. All calibration measurements used NIST calibrated EUV and FUV photodiodes as primary standards and were cross-checked with instrument simulations. More specific information about ground-based calibration of the EUVE Spectrometer may be found in [31] and [14].

In-orbit calibration observations with the Spectrometer were made each month during the first two years after launch, and continue as needed. The Spectrometer wavelength scale, and the imaging and effective areas of all EUVE instruments are monitored on an ongoing basis. Measurements of the DS/S boresight position are made using the positions of images in the Deep Survey instrument. Early results of in-orbit calibrations are summarized in [5]. The instrument characteristics given in Chapter 3 and available in tabular form from the CEA *ftp* site represent the most recent results of instrument monitoring in the areas discussed below.

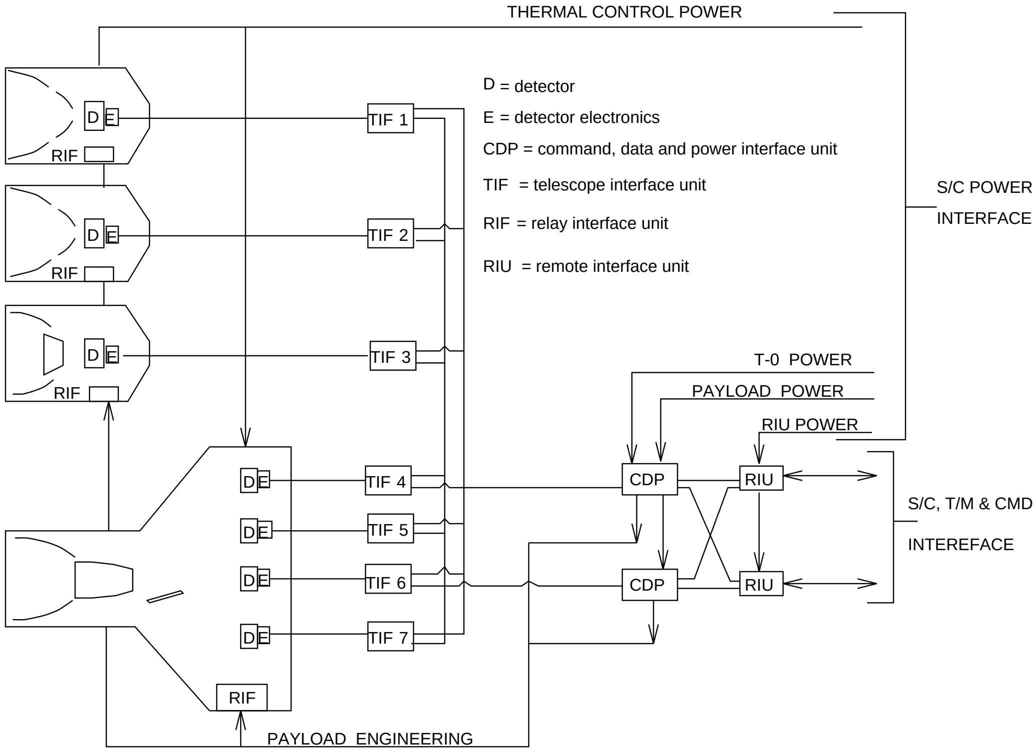

Figure 2-10: EUVE science payload electronics block diagram

2.2.5.1 Effective Area Calibration

Because of the lack of "standard stars" in the EUV, effective areas for the Spectrometer are determined from model spectra for continuum sources. Observations of white dwarf stars provide the baseline measurements. Calibration targets are selected to minimize order confusion. After spectra are extracted, white dwarf model spectra for the object are input to a Spectrometer simulation program, and the model parameters adjusted to produce simulated data that match the observed spectra as nearly as possible. In most cases, the effective temperature and gravity are well constrained by other optical and ultraviolet spectra. The resulting models are then compared whenever possible to photometric and spectroscopic EUV/soft X-ray observations of the same target made with the ROSAT Wide Field Camera, EXOSAT, HUT, IUE, and various rocket experiments. The effective area function is then adjusted to bring the measurements into better agreement. This process is repeated until the effective area function is stable and consistent with accepted error levels in the other measurements.

2.2.5.2 Wavelength Calibration and Spectral Resolution

The above method of arriving at the effective area by comparing spectra relies on an accurate wavelength solution. Spectrometer channel wavelength scales have been calibrated in-orbit by making observations of several well-known line-emission sources before and during the sky survey. Wavelength solutions are determined from line identifications in spectra obtained with both boresight and off-axis pointings during pre-launch and in-orbit calibrations. Polynomial functions of the detector coordinates and the off-axis angles are fit to the observed line positions to produce a wavelength vs. position function. This approach allows the assignment of both a wavelength and a position angle to each photon event, and is independent of aspect correction to a first approximation. An example of an emission spectrum used in the wavelength calibration is plotted in figure 2-11.

2.2.5.3 Spectral Resolution Measurements

The full width at half maximum (FWHM) for a number of unblended lines has been measured in spectra from EUVE calibration observations of late type stars and other emission sources. The results are consistent with pre-launch measurements. These tests check both the spectral resolution of the Spectrometer and the pointing stability of the spacecraft.

2.2.5.4 Polarization

Since grazing incidence reflections tend to be strongly polarizing, polarization in the Spectrometer was measured in pre-launch calibration. As a result of these measurements, some correction for polarization effects in the EUV may be possible[2] for some observations. The Spectrometer throughput for linearly polarized light varies sinusoidally as the instrument is rotated, and the amplitude of the resulting curve characterizes the Spectrometer's response at that wavelength. The modulation is also more pronounced when the polarization vector is oriented radially to the aperture plane (see figure 3-20 for aperture and detector orientations). The throughput amplitude was measured with monochromatic beams of polarized light at a number of wavelengths, and roll angles up to 135 degrees. A simulation of this function, based on Spectrometer raytraces and scaled to bring it into agreement with the calibration measurements, is plotted in figure 2-12. The amplitudes have been normalized by dividing by the average throughput.

[2]Removal of polarization effects is not directly supported by the EGO Center

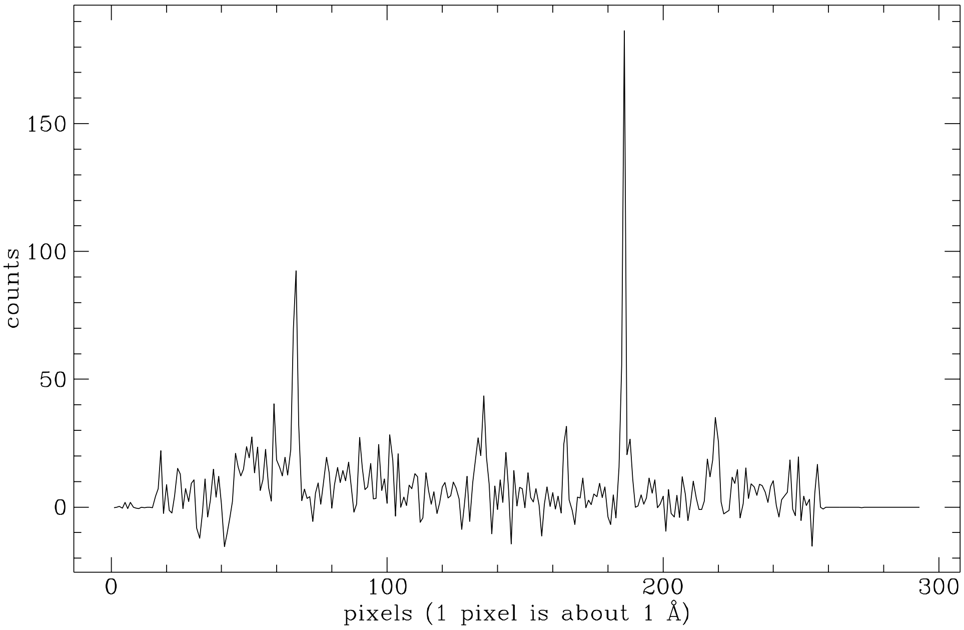

Figure 2-11: SW spectrum of the calibration target AU Mic.

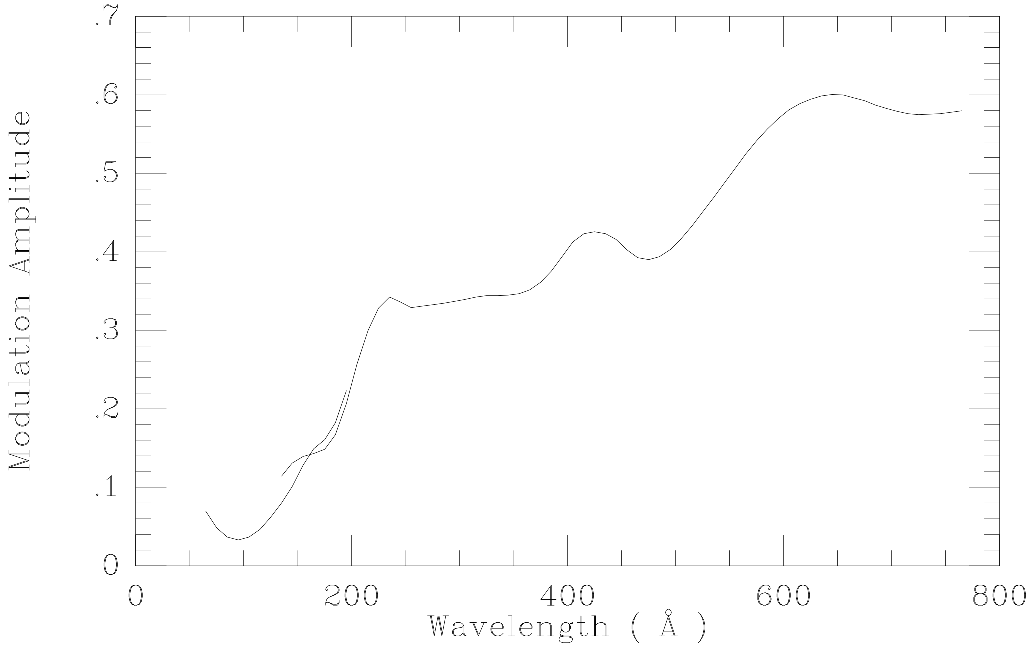

Figure 2-12: Throughput modulation amplitude of a fully polarized source normalized by average throughput. Results of instrument simulation.

2.3 The Deep Survey: an EUV Imaging System

Each of the EUVE survey instruments, is composed of a two-stage grazing incidence mirror, and an MCP detector, with thin film filters. The sky survey instruments (Scanners A, B, and C) are described further in Appendix A. The Deep Survey instrument is a short-wavelength imaging system which takes advantage of the larger geometric area of the DS/S telescope. It is coaxial with the Spectrometer and shares the same mirror assembly.

2.3.0.5 Wavelength Coverage in the Deep Survey Instrument

The Deep Survey instrument operates in a short-wavelength region similar to the bandpasses of Scanners A and B. Its detector is located at the central focus of the DS/S telescope. The detector has a MgF_2 photocathode which enhances quantum efficiency between 50 and 800 Å. The filter is divided into three sections (see figure 2-4). The center section is boron-coated Lexan. Two panels of aluminum and carbon on either side define a second bandpass. Parameters of the detector and filters are listed in table 2-3. Transmissions of the Deep Survey filter materials are shown in figure 2-14. A plot of the effective area, as modeled from pre-launch and in-orbit calibrations, is shown in figure 2-13.

The Deep Survey operates continuously during the pointed phase of the mission. DS Lexan band count rates and image centroids may be used in some data analysis options to help define spacecraft pointing or produce broad band light curves. Obtaining images and count rates in the aluminum/carbon filter during pointed observations will require pointing the DS/S off-axis. However, the instrument PSF degrades considerably for points near the edge of the field of view. Therefore, DS images from the Al/C filters will require longer exposures in proportion to the FWHM, than images from the Lexan filter, to achieve the same photometric signal-to-noise.

2.3.1 Deep Survey Detector Gain

The Deep Survey detector, is known to have developed an area of decreased gain, or "dead spot". This is probably because of extended exposure to very high count rates, during observations of the white dwarf HZ43 in February, 1993. The spot is an area of approximate diameter $\widehat{4'}$ in X by $\widehat{3'}$ in Y, centered at $X = 1033, Y = 1035 \pm 1$, where the quantum efficiency has been degraded by up to 80% at the center. The outer dimensions roughly limit the area with less than 85% of the normal QE. Current strategy to minimize the dead spot's impact on DSS science is to point the instrument off-axis, at an angle which places the DS image outside the areas with the worst gain, while not significantly defocussing either the DS image or the spectrum.

Table 2-3: Deep Survey filters and detector

Deep Survey

Filter Quadrant	**Material**	**Bandpass**	**Broadband MDF**
0 (center)	1498 Å Lexan/1172 Å boron	40–190 Å	2.3 μJy
1,2 (sides)	2039 Å Al/399 Å carbon	160–385 Å	110.0 μJy

Detector Photocathode	MgF_2

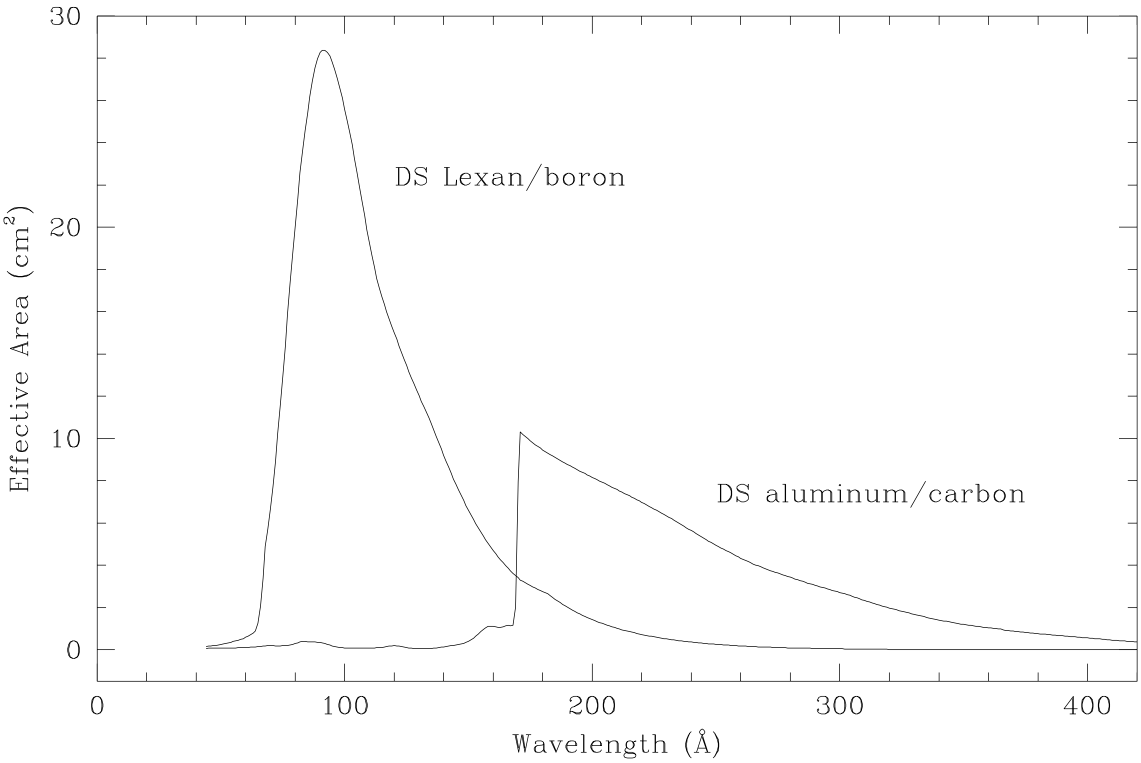

Figure 2-13: Effective areas for the Deep Survey instrument. The shorter wavelength curve is a fit to measurements of the central Lexan/B filter[3]. The longer wavelength curve is derived from measurements of both the Al/C quadrants.

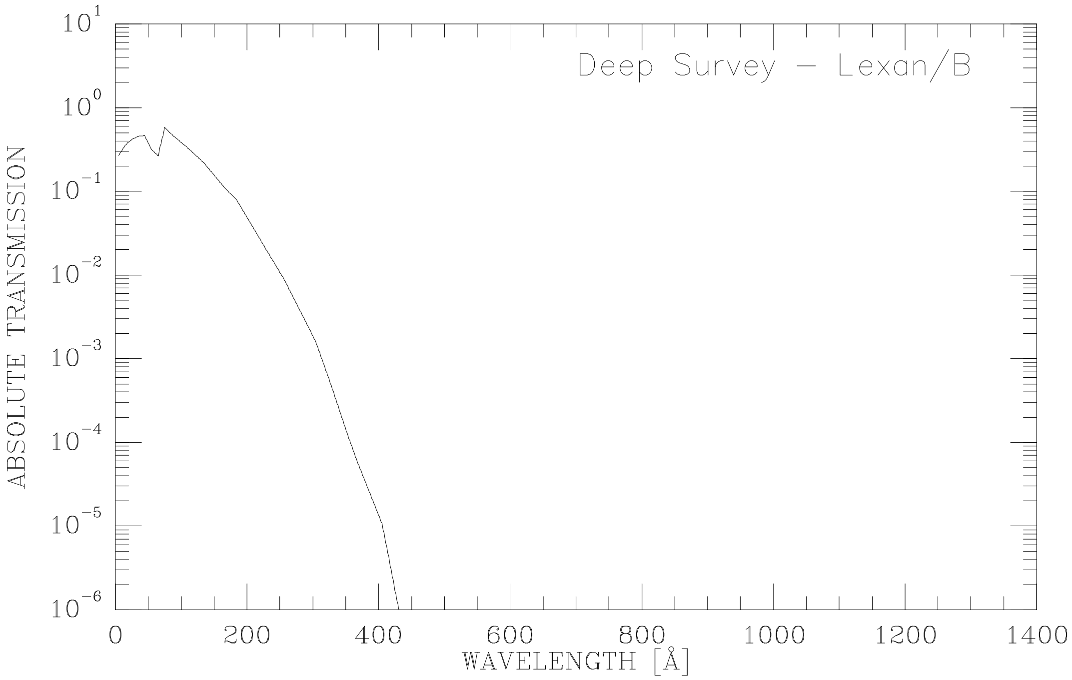

Figure 2-14: a) Deep Survey Lexan filter transmission. Log scale.

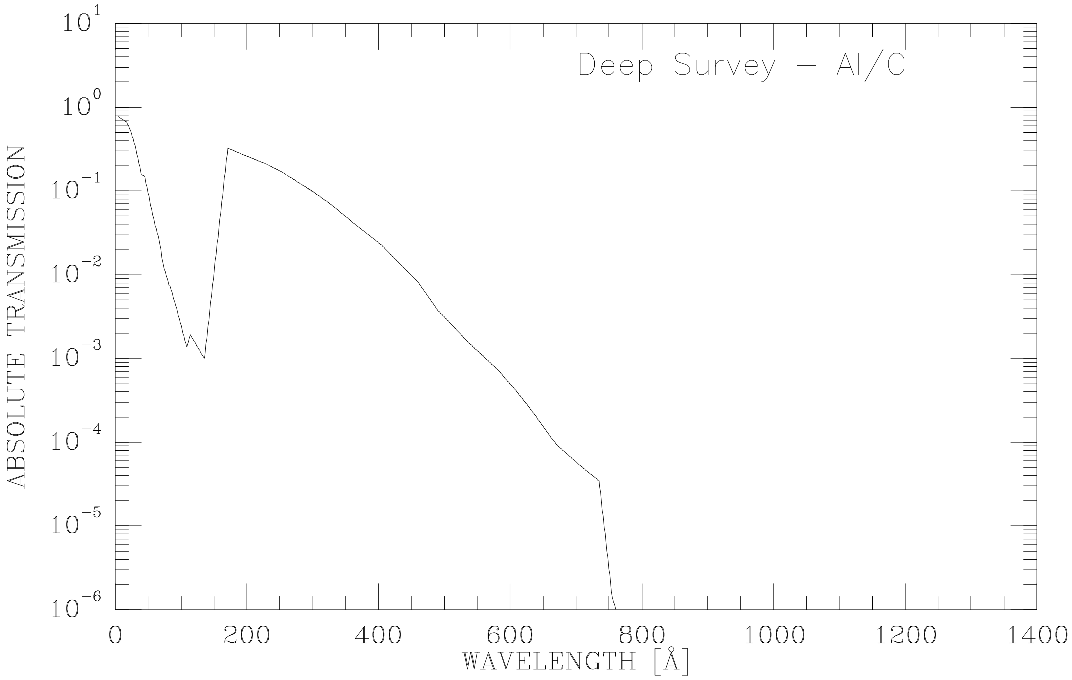

Figure 2-14: b) Deep Survey aluminum/carbon filter transmission. Log scale.